European Conference on Computational Fluid Dynamics
ECCOMAS CFD 2006
P. Wesseling, E. Oñate and J. Périaux (Eds)

FICTITIOUS BOUNDARY AND MOVING MESH METHODS FOR THE NUMERICAL SIMULATION OF PARTICULATE FLOW

D. Anca*, S. Turek† and D. Wan‡

* Institute of Applied Mathematics (LS III), University of Dortmund,
Vogelpothsweg 87, 44227 Dortmund, Germany
e-mail: adan@math.uni-dortmund.de

† Institute of Applied Mathematics (LS III), University of Dortmund,
Vogelpothsweg 87, 44227 Dortmund, Germany
e-mail: ture@featflow.de

‡ School of Naval Architecture, Ocean and Civil Engineering,
Shanghai Jiao Tong University, Huashan Road 1954, 200030, China
e-mail: dcwan@sjtu.edu.cn

Key words: Particulate Flow, Multigrid, FEM, Fictitious Boundary, Moving Mesh

Abstract. *This paper discusses numerical simulation techniques using a moving mesh approach together with the multigrid fictitious boundary method (FBM) for liquid-solid flow configurations. The flow is computed by an ALE formulation with a multigrid finite element solver (FEATFLOW), and the solid particles are allowed to move freely through the computational mesh which can be adaptively aligned by the moving mesh method based on an arbitrary grid. Numerical results show that the presented method can accurately and efficiently handle prototypical particulate flow situations.*

1 INTRODUCTION

Numerical simulation of rigid particulate flows or the motion of small rigid particles in a viscous liquid is one of the main focuses of engineering research and still a challenging task in many applications. Depending on the area of application, these types of problems arise frequently in numerous settings, such as sedimenting and fluidized suspensions, lubricated transport, hydraulic fracturing of reservoirs, slurries, understanding solid-liquid interaction, etc. Several numerical simulation techniques for particulate flow have been developed over the past decade. In these methods, the fluid flow is governed by the continuity and momentum equations, while the particles are governed by the equation of motion for a rigid body. The flow field around each individual particle is resolved so that

the hydrodynamic force between the particle and the fluid can be explicitly obtained. Hu, Joseph and coworkers [1, 2], Galdi [3] and Maury [4] developed a finite element method based on unstructured grids to simulate the motion of rigid particles in Newtonian and viscoelastic fluids. This approach is based on an Arbitrary Lagrangian-Eulerian (ALE) technique. Both the fluid and solid equations of motion are incorporated into a single coupled variational equation. At each time step, a new mesh is generated when the old one becomes too distorted, and the flow field is projected onto the new mesh. In this scheme, the positions of the particles and grid nodes are updated explicitly, while the velocities of the fluid and the solid particles are determined implicitly.

Glowinski, Joseph, Patankar and coauthors [5, 6, 7, 8] proposed a distributed Lagrange multiplier (DLM)/fictitious domain method for the direct numerical simulation of large number of rigid particles in fluids. In the DLM method, the entire fluid-particle domain is assumed to be a fluid and then the particle domain is constrained to move with a rigid motion. The fluid-particle coupling is treated implicitly using a combined weak formulation in which the mutual forces cancel. This formulation permits the use of a fixed structured grid thus eliminating the need for remeshing the domain. Our group [9, 10, 11, 12] presented another multigrid fictitious boundary method (FBM) for the detailed simulation of particulate flows which is based on a fixed unstructured FEM background grid. The motion of the solid particles is modeled by the Newton-Euler equations. Based on the boundary conditions applied at the interface between the particles and the fluid which can be seen as an additional constraint to the governing Navier-Stokes equations, the fluid domain can be extended into the whole domain which covers both fluid and particle domains. An advantage of these fictitious domain methods over the generalized standard Galerkin finite element method is that the fictitious domain methods allow a fixed grid to be used, eliminating the need for remeshing, and they can be handled independently from the flow features. Much progress has been made for adopting the fictitious domain methods to simulate particulate flows, yet the quest for more accurate and efficient methods remains active. An underlying problem when adopting the fictitious domain methods is that the boundary approximation is of low accuracy only. Particularly in three space dimensions, the ability of the fictitious domain methods to deal with the interaction between fluid and rigid particles accurately is greatly limited. One remedy is to preserve the mesh topology, for instance as generalized tensorproduct or blockstructured meshes, while a local alignment with the physical boundary of the solid particles is achieved by a moving mesh process, such that the boundary approximation error can be significantly decreased.

The primary objective of this paper is to combine the multigrid fictitious boundary method (FBM) [9, 11] with the moving mesh method described in [17] for the simulation of particulate flows and to check the accuracy of the proposed combined method. As we have shown in [11], the use of the multigrid FBM does not require to change the mesh during the simulations, although the rigid particles vary their positions. The advantage is that no expensive remeshing has to be performed while a fixed mesh can be used such that

in combination with appropriate data structures and fast CFD solvers very high efficiency rates can be reached. However, the accuracy for capturing the surfaces of solid particles is only of first order which might lead to accuracy problems. For a better approximation of the particle surfaces, we adopt a deformed grid, created from an equidistant cartesian mesh, in which the topology is preserved while only the local grid spacing is changed such that the grid points are concentrated near the surfaces of the rigid particles. Only the solution of additional linear Poisson problems in every time step is required for generating the deformation grid, which means that the additional work is significantly less than the main fluid-particle part. The paper is organized as follows: In Section 2, the physical models together with collision and agglomeration models for the rigid particulate flows are described. The detailed numerical schemes including the multigrid FBM and the moving mesh method are given in Section 3. Numerical experiments are implemented and their computational results will be presented in Section 4. The concluding remarks will be given in Section 5.

2 DESCRIPTIONS OF THE PHYSICAL MODELS

2.1 Governing Equations

In our numerical studies of particle motion in a fluid, we will assume that the fluids are immiscible and Newtonian. The particles are assumed to be rigid. Let us consider the unsteady flow of N particles with mass M_i $(i = 1, \ldots, N)$ in a fluid with density ρ_f and viscosity ν. Denote $\Omega_f(t)$ as the domain occupied by the fluid at time t, and $\Omega_i(t)$ as the domain occupied by the ith particle. So, the motion of an incompressible fluid is governed by the following Navier-Stokes equations in $\Omega_f(t)$,

$$\rho_f \left(\frac{\partial \mathbf{u}}{\partial t} + \mathbf{u} \cdot \nabla \mathbf{u} \right) - \nabla \cdot \sigma = 0 \,, \qquad \nabla \cdot \mathbf{u} = 0 \qquad \forall\, t \in (0, T), \tag{1}$$

where σ is the total stress tensor in the fluid phase defined as

$$\sigma = -p\,\mathbf{I} + \mu_f \left[\nabla \mathbf{u} + (\nabla \mathbf{u})^T \right]. \tag{2}$$

Here, $\mathbf{I}$ is the identity tensor, $\mu_f = \rho_f \cdot \nu$, p is the pressure and $\mathbf{u}$ is the fluid velocity. Let $\Omega_T = \Omega_f(t) \cup \{\Omega_i(t)\}_{i=1}^N$ be the entire computational domain which shall be independent of t. Dirichlet- and Neumann-type boundary conditions can be imposed on the outer boundary $\Gamma = \partial\Omega_f(t)$. Since $\Omega_f = \Omega_f(t)$ and $\Omega_i = \Omega_i(t)$ are always depending on t, we drop t in all following notations. The equations that govern the motion of each particle are the Newton-Euler equations, i.e., the translational velocities $\mathbf{U}_i$ and angular velocities ω_i of the ith particle satisfy

$$M_i \frac{d\,\mathbf{U}_i}{d\,t} = (\Delta M_i)\,\mathbf{g} + \mathbf{F}_i + \mathbf{F}'_i \,, \qquad \mathbf{I}_i \frac{d\,\omega_i}{d\,t} + \omega_i \times (\mathbf{I}_i\,\omega_i) = T_i \,, \tag{3}$$

where M_i is the mass of the ith particle; $\mathbf{I}_i$ is the moment of the inertia tensor; ΔM_i is the mass difference between the mass M_i and the mass of the fluid occupying the same volume; $\mathbf{g}$ is the gravity vector; $\mathbf{F}_i'$ are collision forces acting on the ith particle due to other particles which come close to each other. We assume that the particles are smooth without tangential forces of collisions acting on them; the details of the collision model will be discussed in the following subsection. $\mathbf{F}_i$ and T_i are the resultants of the hydrodynamic forces and the torque about the center of mass acting on the ith particle which are calculated by

$$\mathbf{F}_i = (-1)\int_{\partial\Omega_i} \sigma\cdot\mathbf{n}\, d\,\Gamma_i\,, \qquad T_i = (-1)\int_{\partial\Omega_i} (\mathbf{X}-\mathbf{X}_i)\times(\sigma\cdot\mathbf{n})\; d\,\Gamma_i, \tag{4}$$

where σ is the total stress tensor in the fluid phase defined by Eq. (2), $\mathbf{X}_i$ is the position of the mass center of the ith particle, $\partial\Omega_i$ is the boundary of the ith particle, $\mathbf{n}$ is the unit normal vector on the boundary $\partial\Omega_i$ pointing outward to the flow region. The position $\mathbf{X}_i$ of the ith particle and its angle θ_i are obtained by integration of the kinematic equations

$$\frac{d\,\mathbf{X}_i}{d\,t} = \mathbf{U}_i\,, \qquad \frac{d\,\theta_i}{d\,t} = \omega_i. \tag{5}$$

No-slip boundary conditions are applied at the interface $\partial\Omega_i$ between the ith particle and the fluid, i.e., for any $\mathbf{X}\in\bar{\Omega}_i$, the velocity $\mathbf{u}(\mathbf{X})$ is defined by

$$\mathbf{u}(\mathbf{X}) = \mathbf{U}_i + \omega_i\times(\mathbf{X}-\mathbf{X}_i)\,. \tag{6}$$

2.2 Collision and Agglomeration Models

Following existing modeling approaches, we examine a special collision model with a new definition of short range repulsive forces which can not only prevent the particles from getting too close, it can also deal with the case of particles overlapping each other when numerical simulations bring the particles very close due to unavoidable numerical truncation errors. For the particle-particle collisions, the corresponding repulsive force is determined as

$$\mathbf{F}_{i,j}^P = \begin{cases} 0, & \text{for } \; d_{i,j} > R_i + R_j + \rho, \\ \frac{1}{\epsilon_P'}(\mathbf{X}_i-\mathbf{X}_j)(R_i+R_j-d_{i,j}), & \text{for } \; d_{i,j} < R_i + R_j, \\ \frac{1}{\epsilon_P}(\mathbf{X}_i-\mathbf{X}_j)(R_i+R_j+\rho-d_{i,j})^2, & \text{for } \; R_i+R_j \le d_{i,j} \le R_i+R_j+\rho, \end{cases} \tag{7}$$

where R_i and R_j are the radius of the ith and jth particle, $\mathbf{X}_i$ and $\mathbf{X}_j$ are the coordinates of their mass centers, $d_{i,j} = |\mathbf{X}_i - \mathbf{X}_j|$ is the distance between their mass centers, ρ is the range of the repulsive force (usually $\rho = 0.5 \sim 2.5\Delta h$, Δh is the mesh size), ϵ_P and ϵ_P' are small positive stiffness parameters for particle-particle collisions. If the fluid is sufficiently viscous, and $\rho \simeq \Delta h$ as well as ρ_i/ρ_f are of order 1 (ρ_i is the density of the ith particle,

ρ_f is the fluid density), then we can take $\epsilon_P \simeq (\Delta h)^2$ and $\epsilon'_P \simeq \Delta h$ in the calculations. For the particle-wall collisions, the corresponding repulsive force reads

$$\mathbf{F}_i^W = \begin{cases} 0, & \text{for } \; d'_i > 2R_i + \rho, \\ \frac{1}{\epsilon'_W}(\mathbf{X}_i - \mathbf{X}'_i)(2R_i - d'_i), & \text{for } \; d'_i < 2R_i, \\ \frac{1}{\epsilon_W}(\mathbf{X}_i - \mathbf{X}'_i)(2R_i + \rho - d'_i)^2, & \text{for } \; 2R_i \le d'_i \le 2R_i + \rho, \end{cases} \tag{8}$$

where $\mathbf{X}'_i$ is the coordinate vector of the center of the nearest imaginary particle P'_i located on the boundary wall Γ w.r.t. the ith particle, $d'_i = |\mathbf{X}_i - \mathbf{X}'_i|$ is the distance between the mass centers of the ith particle and the center of the imaginary particle P'_i, ϵ_W is a small positive stiffness parameter for particle-wall collisions, usually it can be taken as $\epsilon_W = \epsilon_P/2$ and $\epsilon'_W = \epsilon'_P/2$ in the calculations. Then, the total repulsive forces (i.e. collision forces) exerted on the ith particle by the other particles and the walls can be expressed as follows,

$$\mathbf{F}'_i = \sum_{j=1, j\neq i}^{N} \mathbf{F}_{i,j}^P + \mathbf{F}_i^W \, . \tag{9}$$

Future plans for this research include also the development of an agglomeration model. As a first step in this direction, we perform a 'trick' to the described collision model such that we obtain a prototypical agglomeration model: Switching the sign for the forces defined, that means instead of a positive sign we put a negative, in this manner the repulsive forces become attractive forces. The result is that the particles will not separate when they touch each other, but they will stick together. At the end of this paper, we will provide preliminary results for this simple agglomeration model while the development of more sophisticated agglomeration models is part of current research.

3 NUMERICAL METHOD

3.1 Multigrid FEM Fictitious Boundary Method

The multigrid FEM fictitious boundary method (FBM) [9, 10, 11] is based on a multigrid FEM background grid which covers the whole computational domain Ω_T and can be chosen independently from the particles of arbitrary shape, size and number. It starts with a coarse mesh which may already contain many of the geometrical details of Ω_i $(i = 1, \ldots, N)$, and it employs a fictitious boundary indicator (see [9]) which sufficiently describes all fine-scale structures of the particles with regard to the fluid-particle matching conditions of Eq. (6). Then, all fine-scale features of the particles are treated as interior objects such that the corresponding components in all matrices and vectors are unknown degrees of freedom which are implicitly incorporated into all iterative solution steps (see [10]). Hence, by making use of Eq. (6), we can perform calculations for the fluid in the whole domain Ω_T. The considerable advantage of the multigrid FBM is that the total mixture domain Ω_T does not have to change in time, and can be meshed only

once. The domain of definition of the fluid velocity $\mathbf{u}$ is extended according to Eq. (6), which can be seen as an additional constraint to the Navier-Stokes equations (1), i.e.,

$$\begin{cases} \nabla \cdot \mathbf{u} = 0 & (a) \quad \text{for} \quad \mathbf{X} \in \Omega_T, \\ \rho_f \left(\frac{\partial \mathbf{u}}{\partial t} + \mathbf{u} \cdot \nabla \mathbf{u} \right) - \nabla \cdot \sigma = 0 & (b) \quad \text{for} \quad \mathbf{X} \in \Omega_f, \\ \mathbf{u}(\mathbf{X}) = \mathbf{U}_i + \omega_i \times (\mathbf{X} - \mathbf{X}_i) & (c) \quad \text{for} \quad \mathbf{X} \in \bar{\Omega}_i, \ i = 1, \ldots, N. \end{cases} \tag{10}$$

For the study of interactions between the fluid and the particles, the calculation of the hydrodynamic forces acting on the moving particles is very important. From Eq. (4), we can see that the surface integrals on the wall surfaces of the particles should be conducted for the calculation of the forces $\mathbf{F}_i$ and T_i. However, in the presented multigrid FBM method, the shapes of the wall surface of the moving particles are implicitly imposed in the fluid field. If we reconstruct the shapes of the wall surface of the particles, it is not only a time consuming work, but also the accuracy is only of first order due to a piecewise constant interpolation from our indicator function. For overcoming this problem, we perform the hydrodynamic force calculations using a volume based integral formulation. To replace the surface integral in Eq. (4) we introduce a function α_i,

$$\alpha_i(\mathbf{X}) = \begin{cases} 1 & \text{for} \quad \mathbf{X} \in \Omega_i, \\ 0 & \text{for} \quad \mathbf{X} \in \Omega_T \setminus \Omega_i, \end{cases} \tag{11}$$

where $\mathbf{X}$ denotes the coordinates. The importance of such a definition can be seen from the fact that the gradient of α_i is zero everywhere except at the wall surface of the ith particle, and equals to the normal vector $\mathbf{n}_i$ of wall surface of the ith particle defined on the grid, i.e., $\mathbf{n}_i = \nabla \alpha_i$. Then, the hydrodynamic forces acting on the ith particle can be computed by

$$\mathbf{F}_i = -\int_{\Omega_T} \sigma \cdot \nabla \alpha_i \, d\,\Omega, \, , \qquad T_i = -\int_{\Omega_T} (\mathbf{X} - \mathbf{X}_i) \times (\sigma \cdot \nabla \alpha_i) \, d\,\Omega \, . \tag{12}$$

The integral over each element covering the whole domain Ω_T can be exactly calculated with a standard Gaussian quadrature of sufficiently high order. Since the gradient $\nabla \alpha_i$ is non-zero only near the wall surface of the ith particle, thus the volume integrals need to be computed only in one layer of mesh cells around the ith particle, which leads to a very efficient treatment.

The algorithm of the multigrid FEM fictitious boundary method for solving the coupled system of fluid and particles can be summarized as follows:

1. Given the positions and velocities of the particles, solve the fluid equations Eqs. (10) (a) and (b) in the corresponding fluid domain involving the position of the particles for the fictitious boundary conditions.

2. Calculate the corresponding hydrodynamic forces and the torque acting on the particles by using Eq. (12), and compute the collision forces by Eq. (9).

3. Solve Eq. (3) to get the translational and angular velocities of the particles, and then obtain the new positions and velocities of the particles by Eq. (5).

4. Use Eq. (10) (c) to set the new fluid domain and fictitious boundary conditions, and then advance to solve for the new velocity and pressure of the fluid phase as described in step 1.

3.2 Moving Mesh Method

In this subsection, we briefly describe the moving mesh method which will be adopted and coupled with above multigrid fictitious boundary method (FBM) to solve numerically the particulate flows. The details of the moving mesh method can be found in Ref. [17].

The moving mesh problem can be equated to constructing a transformation φ, $x = \varphi(\xi)$ from computational space (with coordinate ξ) to physical space (with coordinate x). There are two basic types of moving mesh methods, generally computing x by minimizing a variational form or computing the mesh velocity $v = x_t$ using a Lagrangian like formulation. The applied moving mesh method belongs to the velocity based methods, which is based on Liao's [13, 14, 15, 16] and Moser's work [18]. This method has several advantages: only linear Poisson problems on fixed meshes are needed to be solved, monitor functions can be obtained directly from error distributions or distance functions, mesh tangling can be prevented, and the data structure for the mesh nodes is always the same as for the starting mesh.

Suppose $g(x)$ (area function) to be the area distribution on the undeformed mesh, while $f(x)$ (monitor function) describes the absolute mesh size distribution of the target grid, which is independent of the starting grid and chosen according to the need of physical problems. Then, the transformation φ can be computed via the following four steps:

1. Compute the scale factors c_f and c_g for the given monitor function $f(x) > 0$ and the area function g using

$$c_f \int_\Omega \frac{1}{f(x)} dx = c_g \int_\Omega \frac{1}{g(x)} dx = |\Omega|, \tag{13}$$

where Ω is the computational domain, and $f(x) \approx$ local mesh area. Let $\tilde{f}$ and $\tilde{g}$ denote the reciprocals of the scaled functions f and g, i.e.,

$$\tilde{f} = \frac{c_f}{f}, \qquad \tilde{g} = \frac{c_g}{g}. \tag{14}$$

2. Compute a grid-velocity vector field $v : \Omega \to \mathbf{R}^n$ by satisfying the following linear Poisson problem

$$-\mathrm{div}(v(x)) = \tilde{f}(x) - \tilde{g}(x), \quad x \in \Omega, \quad \text{and} \quad v(x) \cdot \mathbf{n} = 0, \quad x \in \partial\Omega, \tag{15}$$

where $\mathbf{n}$ being the outer normal vector of the domain boundary $\partial\Omega$, which may consist of several boundary components.

3. For each grid point x, solve the following ODE system

$$\frac{\partial \varphi(x,t)}{\partial t} = \eta(\varphi(x,t),t), \quad 0 \le t \le 1, \quad \varphi(x,0) = x, \tag{16}$$

with

$$\eta(y,s) := \frac{v(y)}{s\tilde{f}(y) + (1-s)\tilde{g}(y)}, \quad y \in \Omega, \;\; s \in [0,1]. \tag{17}$$

4. Get the new grid points via

$$\varphi(x) := \varphi(x,1). \tag{18}$$

3.3 ALE Formulation of the FBM

For a better approximation of the solid surfaces, we adopt the above described moving mesh method such that we can preserve the mesh topology as generalized tensorproduct or blockstructured meshes, while a local alignment with the rigid body surface is reached. The moving mesh method is sometimes referred to as the quasi-Lagrangian method. When the moving mesh method is applied to the multigrid FBM, a mesh velocity $\mathbf{W}_m$ in the convective term in Eq. (10b) should be introduced, i.e.,

$$\rho_f \left[\frac{\partial \mathbf{u}}{\partial t} + (\mathbf{u} - \mathbf{W}_m) \cdot \nabla \mathbf{u} \right] - \nabla \cdot \sigma = 0 \qquad \text{for} \;\; \mathbf{X} \in \Omega_f. \tag{19}$$

In the literature this is also referred to as an Arbitrary Lagrangian-Eulerian (ALE) formulation. Note that the mesh velocities $\mathbf{W}_m$ do not appear in the continuity equation since a pressure-Poisson equation is solved to satisfy the continuity equation in an outer loop. Care has to be taken to satisfy the geometric conservation law (GCL), where the mesh velocity $\mathbf{W}_m$ must be equal to the movement of the mesh velocity $\Delta\mathbf{x}$ during the time step. Therefore, the mesh velocities $\mathbf{W}_m$ should be calculated according to the nodal movement from the previous time step by

$$\mathbf{W}_m = \frac{1}{\Delta t}(\mathbf{x}^{n+1} - \mathbf{x}^n) \tag{20}$$

where Δt is the time step size and n denotes the time step number. In each time step, a new deformation mesh is generated based on a starting equidistance mesh, then the system matrices are updated and the mesh velocity according to the new position of the deformation mesh nodes should be calculated.

3.4 Time Discretization by Fractional-Step-θ Scheme

The fractional-step-θ scheme is a strongly A-stable time stepping approach which possesses the full smoothing property being important in the case of rough initial or boundary data. It also contains only very little numerical dissipation which is crucial in the computation of non-enforced temporal oscillations. A more detailed discussion of these aspects can be found in [19, 20]. We first semi-discretize the Eqs. (10) (a) and (19) in time by the fractional-step-θ scheme. Given $\mathbf{u}^n$ and the time step $K = t_{n+1} - t_n$, then solve for $\mathbf{u} = \mathbf{u}^{n+1}$ and $p = p^{n+1}$. In the fractional-step-θ-scheme, one macro time step $t_n \rightarrow t_{n+1} = t_n + K$ is split into three consecutive substeps with $\tilde{\theta} := \alpha\theta K = \beta\theta' K$,

$$\begin{aligned}
[I + \tilde{\theta}N(\mathbf{u}^{n+\theta})]\mathbf{u}^{n+\theta} + \theta K \nabla p^{n+\theta} &= [I - \beta\theta K N(\mathbf{u}^n)]\mathbf{u}^n \\
\nabla\cdot\mathbf{u}^{n+\theta} &= 0\,, \\
[I + \tilde{\theta}N(\mathbf{u}^{n+1-\theta})]\mathbf{u}^{n+1-\theta} + \theta' K \nabla p^{n+1-\theta} &= [I - \alpha\theta' K N(\mathbf{u}^{n+\theta})]\mathbf{u}^{n+\theta} \\
\nabla\cdot\mathbf{u}^{n+1-\theta} &= 0\,, \\
[I + \tilde{\theta}N(\mathbf{u}^{n+1})]\mathbf{u}^{n+1} + \theta K \nabla p^{n+1} &= [I - \beta\theta K N(\mathbf{u}^{n+1-\theta})]\mathbf{u}^{n+1-\theta} \\
\nabla\cdot\mathbf{u}^{n+1} &= 0\,,
\end{aligned} \tag{21}$$

where $\theta = 1 - \frac{\sqrt{2}}{2}$, $\theta' = 1 - 2\theta$, and $\alpha = \frac{1-2\theta}{1-\theta}$, $\beta = 1 - \alpha$, $N(\mathbf{v})\mathbf{u}$ is a compact form for the diffusive and convective part,

$$N(\mathbf{v})\mathbf{u} := -\nu\ \nabla\cdot\ \left[\nabla\mathbf{u} + (\nabla\mathbf{u})^T\right] + (\mathbf{v} - \mathbf{W}_m)\cdot\nabla\mathbf{u}\,. \tag{22}$$

Therefore, from Eq. (21), in each time step we have to solve nonlinear problems of the following type,

$$[I + \theta_1 K N(\mathbf{u})]\mathbf{u} + \theta_2 K\nabla p = \mathbf{f}\,, \quad \mathbf{f} := [I - \theta_3 K N(\mathbf{u}^n)]\mathbf{u}^n\,, \ \ \nabla\cdot\mathbf{u} = 0\,. \tag{23}$$

For the Eq. (10) (c), we simply take an explicit expression, that means

$$\mathbf{u}^{n+1} = \mathbf{U}_i^n + \omega_i^n \times (\mathbf{X}^n - \mathbf{X}_i^n)\,. \tag{24}$$

3.5 Space Discretization by Finite Element Method

If we define a pair $\{\mathbf{u}, p\} \in H := \mathbf{H}_0^1(\Omega) \times L := \mathrm{L}_0^2(\Omega)$, and bilinear forms $a(\mathbf{u}, \mathbf{v}) := (\nabla\mathbf{u}, \nabla\mathbf{v})$ and $b(p, \mathbf{v}) := -(p, \nabla\cdot\mathbf{v})$, a weak formulation of the Eq. (23) reads as follows:

$$\begin{cases} (\mathbf{u}, \mathbf{v}) + \theta_1 K\,[\,a(\mathbf{u}, \mathbf{v}) + n(\mathbf{u}, \mathbf{u}, \mathbf{v})\,] + \theta_2 K\, b\,(p, \mathbf{v}) = (\mathbf{f}, \mathbf{v}) & \forall\,\mathbf{v} \in H \\ b\,(q, \mathbf{u}) = 0 & \forall\, q \in L \end{cases} \tag{25}$$

Here, $\mathrm{L}_0^2(\Omega)$ and $\mathbf{H}_0^1(\Omega)$ are the usual Lebesgue and Sobolev spaces, $n(\mathbf{u}, \mathbf{u}, \mathbf{v})$ is a trilinear form defined by

$$n(\mathbf{u}, \mathbf{v}, \mathbf{w}) := \int_\Omega [u_i - (W_m)_i] \left(\frac{\partial v_j}{\partial x_i} + \frac{\partial v_i}{\partial x_j}\right) w_j\, dx\,. \tag{26}$$

To discretize Eq. (25) in space, we introduce a regular finite element mesh T_h consisting of quadrilaterals to cover the whole computational domain, where h is the symbol used as a parameter characterizing the maximum width of the elements of T_h. To obtain the fine mesh T_h from a coarse mesh T_{2h}, we simply connect opposing midpoints. In the fine grid T_h, the old midpoints of the coarse mesh T_{2h} become vertices. We choose $\tilde{Q}1/Q0$ element pair which uses rotated bilinear shape function for the velocity spanned by $\langle x^2 - y^2, x, y, 1\rangle$ in 2D and piecewise constants for the pressure in cells. The nodal values are the mean values of the velocity vector over the element edges, and the mean values of the pressure over the elements. The nonconforming $\tilde{Q}1/Q0$ element pair has several important features. It satisfies the Babuška–Brezzi condition without any additional stabilization, and the stability constant is independent of the shape and size of the element. In particular on meshes containing highly stretched and anisotropic cells, the stability and the approximation properties are always satisfied [19]. If we choose finite-dimensional spaces H_h and L_h and define a pair $\{\mathbf{u}_h, p_h\} \in H_h \times L_h$, the discrete problem of Eq. (25) reads,

$$\begin{cases} (\mathbf{u}_h, \mathbf{v}_h) + \theta_1 K \left[a_h(\mathbf{u}_h, \mathbf{v}_h) + \tilde{n}_h(\mathbf{u}_h, \mathbf{u}_h, \mathbf{v}_h) \right] \\ \qquad\qquad + \theta_2 K\, b_h(p_h, \mathbf{v}_h) = (\mathbf{f}, \mathbf{v}_h)\,, & \forall\, \mathbf{v}_h \in H_h \\ b_h(q_h, \mathbf{u}_h) = 0\,, & \forall\, q_h \in L_h \end{cases} \tag{27}$$

where $a_h(\mathbf{u}_h, \mathbf{v}_h) := \sum_{T\in T_h} a(\mathbf{u}_h, \mathbf{v}_h)_{|T}$ and $b_h(p_h, \mathbf{v}_h) := \sum_{T\in T_h} b(p_h, \mathbf{v}_h)_{|T}$. Note that $\tilde{n}_h(\mathbf{u}_h, \mathbf{u}_h, \mathbf{v}_h)$ is a new convective term which includes streamline-diffusion stabilizations defined by

$$\tilde{n}_h(\mathbf{u}_h, \mathbf{v}_h, \mathbf{w}_h) := \sum_{T\in T_h} n(\mathbf{u}_h, \mathbf{v}_h, \mathbf{w}_h)_{|T} + \sum_{T\in T_h} \delta_T(\mathbf{u}_h \cdot \nabla \mathbf{v}_h, \mathbf{u}_h \cdot \nabla \mathbf{w}_h)_{|T}\,, \tag{28}$$

here δ_T is a local artificial viscosity which is a function of a local Reynolds number Re_T,

$$\delta_T := \delta^* \cdot \frac{h_T}{||\mathbf{u}||_\Omega} \cdot \frac{2Re_T}{1 + Re_T}\,, \qquad Re_T = \frac{||\mathbf{u}||_T \cdot h_T}{\nu}\,, \tag{29}$$

where $||\mathbf{u}||_\Omega$ means the maximum norm of velocity in Ω_T, $||\mathbf{u}||_T$ is an averaged norm of velocity over T, h_T denotes local mesh size of T, and δ^* is an additional free parameter which can be chosen arbitrarily ($\delta^* = 0.1$ is used in our calculations, also see [19]). Obviously, for small local Reynolds numbers, with $Re_T \to 0$, δ_T is decreasing such that we reach in the limit case the standard second order central discretization. Vice versa, for convection dominated flows with $Re_T >> 1$, we add an anisotropic diffusion term of size $O(h)$ which is aligned to the streamline direction $\mathbf{u}_h$.

4 NUMERICAL RESULTS

First, the case of a single moving particle in the fluid is presented to validate the improvement of accuracy and efficiency through the presented mesh deformation method.

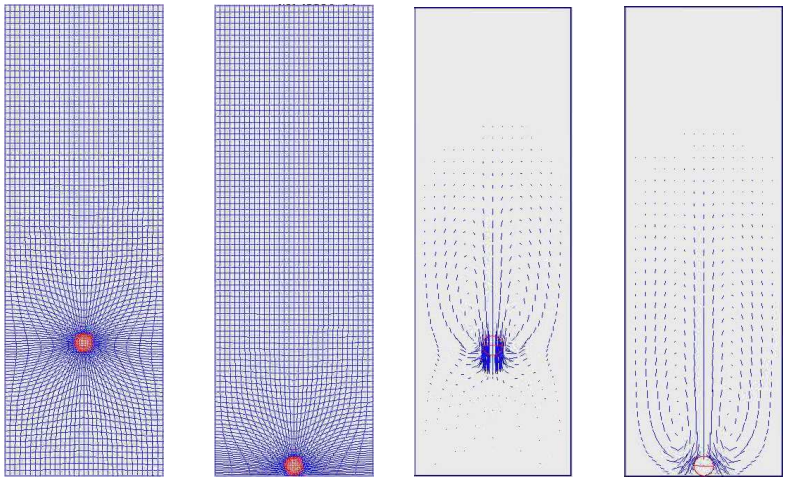

(a) $t = 0.30$ (b) $t = 0.48$ (c) $t = 0.30$ (d) $t = 0.48$

Figure 1: One 2D circular ball falling down in a channel

Moreover, the drafting, kissing and tumbling of two balls in a channel and results for the agglomeration model applied to two particles are provided to demonstrate that the presented method can be easily applied to particulate flows with several particles.

4.1 One 2D Circular Ball Falling Down in a Channel

The (non-dimensional) computational domain is a channel of width 2 and height 6. A circular ball with diameter $d = 0.25$ and density $\rho_p = 1.5$ is located at $(1, 4)$ at time $t = 0$, and it is falling down under gravity in an incompressible fluid with density $\rho_f = 1$ and viscosity $\nu = 0.1$, the gravitational constant is $g = -980$. We suppose that the ball and the fluid are initially at rest. The simulation is carried out on fixed equidistant meshes and moving deformation meshes, respectively, each of them having two different level, i.e., Level = 6 with 12545 nodes and 12288 elements, as well as Level = 7 with 49665 nodes and 49152 elements. Fig. 1 gives two 'snapshots' at $t = 0.30$ and $t = 0.48$ of the deformed meshes and vector fields, respectively. Fig. 2 presents the comparison of the time history of the y-coordinate and the v-component velocity of the center of the ball by using equidistant meshes and deformation meshes, each of them is calculated on the two mesh levels LEVEL = 6 and LEVEL = 7, respectively. If we compare these results with those obtained by Glowinski in Ref. [8], we can find the results of the deformation meshes are much closer to Glowinski's results than the ones on the equidistant meshes, which shows the expected higher accuracy and efficiency.

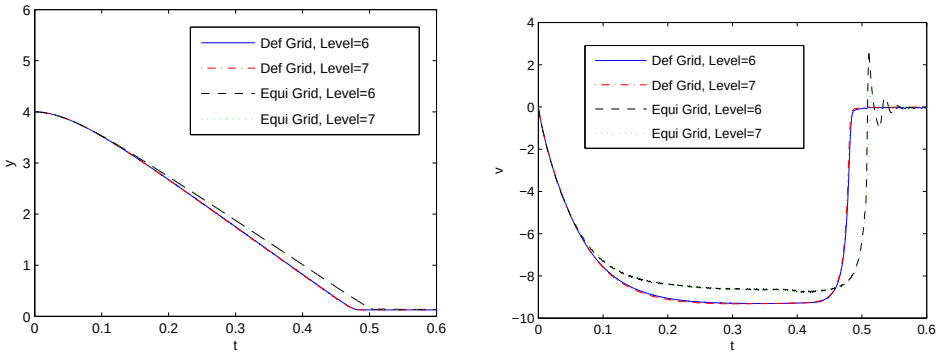

(a) $y \sim t$ (b) $v \sim t$

Figure 2: The time history of y and v of the center of a 2D ball falling down in a channel

4.2 Drafting, Kissing and Tumbling of Two Disks in a Channel

In the following two numerical experiments, we will analyze the case of several moving particles in a fluid. When two particles are dropped closely to each other, they interact by undergoing "drafting, kissing and tumbling" [21], which is often chosen to examine the complete computational model of particulate flows, including the prevention of collisions. Therefore, we also study the sedimentation of two circular particles in a two-dimensional channel, comparing the results with respect to two different level of grid deformation mesh sizes and regarding the results in [8]. The computational domain is a channel of width 2 and height 6. Two rigid circular disks with diameter $d = 0.25$ and density $\rho_p = 1.5$ are located at $(1, 5)$ (No.1 disk) and $(1, 4.5)$ (No.2 disk) at time $t = 0$, and they are falling down under gravity in an incompressible fluid with density $\rho_f = 1$ and viscosity $\nu = 0.01$. We suppose that the disks and the fluid are initially at rest. The simulation is carried out on the time-dependent deformation meshes, having two different level, i.e., Level = 7 with 49665 nodes and 49152 elements, as well as Level = 8 with 197633 nodes and 196608 elements.

Fig. 3 shows the moving deformation meshes employed in the simulation of the two falling disks. The grid lines are always concentrated around the surfaces of the two disks and in the region of the gap between the two disks, and move with the two disks during the computations. From these figures, we can see that the disk in the wake (No.1 particle) falls more rapidly than the disk No.2 in front since the fluid forces acting on it are smaller. The gap between them decreases, and they almost touch ("kiss") each other at time $t = 0.15$. After touching, the two disks fall together until they tumble ($t = 0.18$) and subsequently they separate from each other ($t = 0.30$). The tumbling of the disks takes place because the configuration, when both are parallel to the flow direction, is unstable. The No.1 disk is touching first the bottom wall at $t = 0.42$, while the No.2 disk reaches the bottom wall at $t = 0.65$. All results compare qualitatively well with those presented in [6, 8, 22, 23].

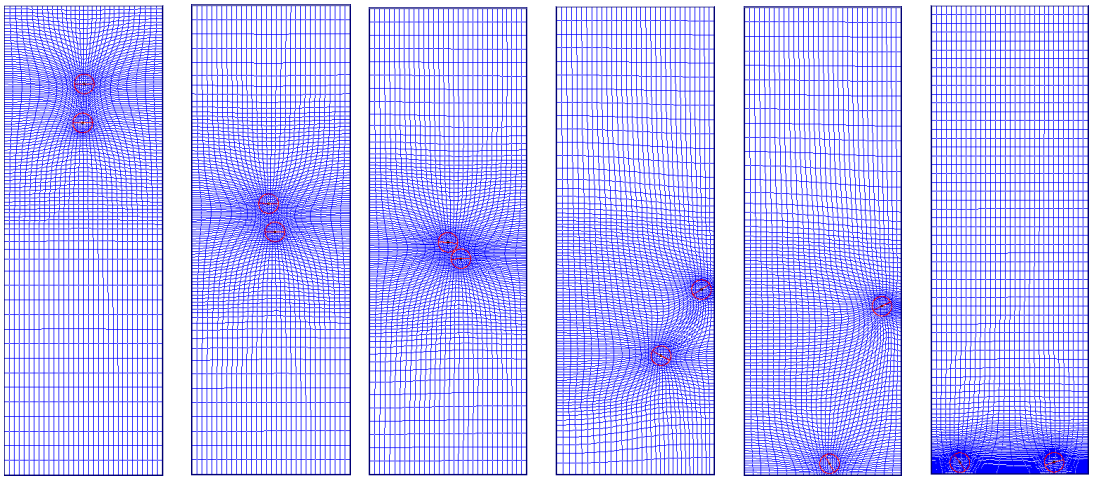

(a) $t = 0.0$ (b) $t = 0.15$ (c) $t = 0.18$ (d) $t = 0.30$ (e) $t = 0.42$ (f) $t = 0.65$

Figure 3: Deformation meshes for two circular disks falling down in an (infinite) channel

4.3 Agglomeration results

As we have described earlier, we also provide numerical results regarding the proposed simple agglomeration model. So, we start with two circular disks, very close one to each other, in the middle part of a channel with width 2 and height 6 which is assumed to be part of an infinite channel. Fig. 4 shows how the particles behave: We can observe that the particles come very close to each other, then they touch and they remain connected. Future research activities are to develop much more sophisticated agglomeration models.

5 Conclusions

We have presented the combination of the multigrid fictitious boundary method and a special moving mesh method for the simulation of particulate flow with moving rigid particles. The new approach directly improves the accuracy upon the previous pure multigrid FBM for particulate flows on fixed grids. It is also computationally cheap and simple to implement. Since the size of the problem and the data structure are fixed, this enables the proposed method to be incorporated into most CFD codes without the need for changing of data structures and special interpolation procedures. It is suitable to accurately and efficiently perform the direct numerical simulation of particulate flows, also for larger numbers of moving particles. Numerical examples of single moving particles in a fluid as well as the drafting, kissing and tumbling of two balls in a channel have been presented to show that the described method can significantly improve the accuracy for dealing with the interaction between the fluid and the particles. Additionally, we presented preliminary numerical results for two disks in a channel using a simple, but prototypical agglomeration model which will be extended in future.

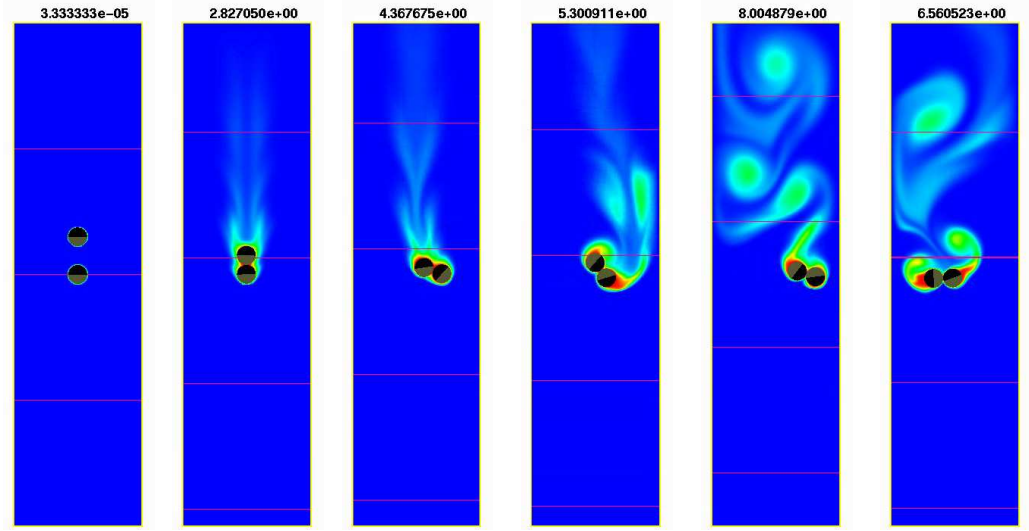

Figure 4: Agglomeration model for two circular disk falling down in a channel

REFERENCES

[1] Hu, H.H., Joseph, D.D., Crochet, M.J.: Direct Simulation of Fluid Particle Motions. Theor. Comp. Fluid Dyn., **3**, 285 – 306 (1992)

[2] Hu, H.H., Patankar, N.A., Zhu, M.Y.: Direct Numerical Simulations of Fluid-Solid Systems Using the Arbitrary Lagrangian-Eulerian Techniques. J. Comput. Phys., **169**, 427 – 462 (2001)

[3] Galdi, G.P., Heuveline, V.: Lift and Sedimentation of particles on the Flow of a Viscoelastic Liquid in a Channel (to be published)

[4] Maury, B.: Direct Simulations of 2D Fluid-Particle Flows in Biperiodic Domains. J. Comput. Phy., **156**, 325 – 351 (1999)

[5] Glowinski, R., Pan, T.W., Hesla, T.I., Joseph, D.D.: A Distributed Lagrange Multiplier/Fictitious Domain Method for Particulate Flows. Int. J. Multiphase Flow, **25**, 755 – 794 (1999)

[6] Patankar, N.A., Singh, P., Joseph, D.D., Glowinski, R., Pan, T.W.: A New Formulation of the Distributed Lagrange Multiplier/Fictitious Domain Method for Particulate Flows. Int. J. Multiphase Flow, **26**, 1509 – 1524 (2000)

[7] Glowinski, R., Pan, T.W., Hesla, T.I., Joseph, D.D., Periaux, J.: A Fictitious Domain Approach to the Direct Numerical Simulation of Incompressible Viscous Flow Past Moving Rigid Bodies: Application to Particulate Flow. J. Comput. Phy., **169**, 363 – 426 (2001)

[8] Glowinski, R.: Finite Element Methods for Incompressible Viscous Flow. In *Handbook of numerical analysis*, **Vol. IX**, Ciarlet, P.G and Lions, J.L., Editors, North-Holland, Amsterdam, 701 – 769 (2003)

[9] Turek, S., Wan, D.C., Rivkind, L.S.: The Fictitious Boundary Method for the Implicit Treatment of Dirichlet Boundary Conditions with Applications to Incompressible Flow Simulations. Challenges in Scientific Computing, Lecture Notes in Computational Science and Engineering, Vol. **35**, Springer, 37 – 68 (2003)

[10] Wan, D.C., Turek, S., Rivkind, L.S.: An Efficient Multigrid FEM Solution Technique for Incompressible Flow with Moving Rigid Bodies. Numerical Mathematics and Advanced Applications, ENUMATH 2003, Springer, 844 – 853 (2004)

[11] Wan, D.C., Turek, S.: Direct Numerical Simulation of Particulate Flow via Multigrid FEM Techniques and the Fictitious Boundary Method. Int. J. Numer. Method in Fluids, in press (2006)

[12] Wan, D.C., Turek, S.: An Efficient Multigrid-FEM Method for the Simulation of Liquid-Solid Two Phase Flows. J. for Comput. and Appl. Math., in press (2006)

[13] Bochev, P.B., Liao, G., de la Pena, G.C.: Analysis and Computation of Adaptive Moving Grids by Deformation. Numerical Methods for Partial Differential Equations, **12**, 489 (1996)

[14] Liao, G., Semper, B.: A Moving Grid Finite–Element Method Using Grid Deformation. Numerical Methods for Partial Differential Equations, **11**, 603 – 615 (1995)

[15] Liu, F., Ji, S., Liao, G.: An Adaptive Grid Method and its Application to Steady Euler Flow Calculations. SIAM Journal on Scientific Computing, **20**(3), 811 – 825 (1998)

[16] Cai, X.X., Fleitas, D., Jiang, B., Liao, G.: Adaptive Grid Generation Based on Least–Squares Finite–Element Method. Computers and Mathematics with Applications, **48**(7-8), 1077 – 1086 (2004)

[17] Grajewski, M., Köster, M., Kilian, S., Turek, S.: Numerical Analysis and Practical Aspects of a Robust and Efficient Grid Deformation Method in the Finite Element Context. submitted to SISC (2005)

[18] Dacorogna, B., Moser, J.: On a Partial Differential Equation Involving the Jacobian Determinant. Annales de le Institut Henri Poincare, **7**, 1 – 26 (1990)

[19] Turek, S.: Efficient Solvers for Incompressible Flow Problems. Springer Verlag, Berlin-Heidelberg-New York (1999)

[20] Turek, S.: A comparative study of time stepping techniques for the incompressible Navier–Stokes equations: From fully implicit nonlinear schemes to semi–implicit projection methods, Int. J. Numer. Meth. Fluids, 22, 987 – 1011 (1996)

[21] Fortes, A., Joseph, D.D., Lundgren, T.: Nonlinear mechanics of fluidization of beds of spherical particles, J. Fluid Mech., **177**, 497 – 483 (1987)

[22] Singh, P., Hesla, T.I., Joseph, D.D.: Distributed Lagrange multiplier method for particulate flows with collisions. Int. J. Multiphase Flow, **29**, 495 – 509 (2003)

[23] Diaz-Goano, C., Minev, P., Nandakumar, K.: A Lagrange multiplier/fictitious domain approach to particulate flows, in: Margenov, W., Yalamov (Eds), Lecture Notes in Computer Science, Vol. 2179, Springer, 409 – 422 (2001)